# Detection of Stressful Situations Using GSR While Driving a BCI-controlled Wheelchair

Aniana Cruz[1], Gabriel Pires[1,3], Ana C. Lopes[1,3] and Urbano J. Nunes[1,2]

*Abstract*— This paper analyzes the galvanic skin response (GSR) recorded from healthy and motor disabled people while steering a robotic wheelchair (RobChair ISR-UC prototype), to infer whether GSR can help in the recognition of stressful situations. Seven healthy individuals and six individuals with motor disabilities were asked to drive the RobChair by means of a brain-computer interface in indoor office environments, including complex scenarios such as passing narrow doors, avoiding obstacles, and with situations of unexpected trajectories of the wheelchair (controlled by an operator without users knowledge). All these driving situations can trigger emotional arousals such as anxiety and stress. A method called feature-based peak detection (FBPD) was proposed for automatic detection of skin conductance response (SCR) which proved to be very effective compared to the state-of-the-art methods. We found that SCR was elicited in 100% of the occurrences of collisions (lateral scrapings) and 94% of unexpected trajectories.

## I. INTRODUCTION

Brain-actuated robotic wheelchairs can help individuals with severe motor disabilities to increase their levels of mobility. Several studies have demonstrated that healthy and motor-impaired people can successfully steer a brain-actuated wheelchair, as long as it is supported by a navigation system with a human-machine collaborative controller [1], [2], [3]. Users who drive a robotic wheelchair through a brain computer interface (BCI) provide only sparse commands encoding direction decisions or destinations, while the navigation system is responsible for perceiving the environment, planning and executing the trajectories. Therefore, users know that they do not have a full control of the wheelchair, strongly relying on the machine. This can make them experience stressful reactions such as fear and anxiety, when placed in difficult or unexpected situations (e.g., narrow-door passages or unexpected obstacles). These emotional reactions may eventually contribute to a degradation of the BCI classification performance leading to unwanted navigation commands, which can worsen the stressing situations. Changes in emotional states such as anxiety or fear produce bodily reactions not controlled by the person, which are driven by the sympathetic chain of the autonomic nervous system (ANS) [4]. One such reaction is the increase of the sweat glands activity, resulting in

[1] Institute for Systems and Robotics, University of Coimbra, 3030-290 Coimbra, Portugal  e-mail: `anianabrito@isr.uc.pt`, `gpires@isr.uc.pt`, `anacris@isr.uc.pt` and `urbano@isr.uc.pt`
[2] Department of Electrical and Computer Engineering, University of Coimbra, 3030-290 Coimbra, Portuga
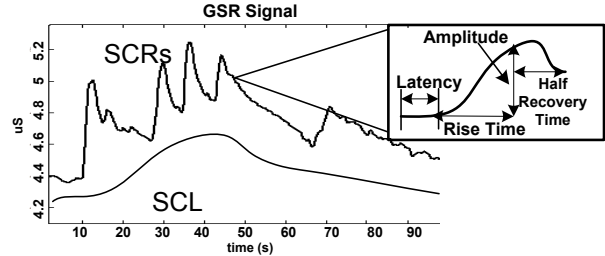[3] Polytechnic Institute of Tomar, 2300-313 Tomar, Portugal

Fig. 1. Skin conductance responses (SCRs) and skin conductance level (SCL) of a typical GSR signal (filtered by a low-pass filter at 1 Hz).

increased skin conductance. Thus, galvanic skin response (GSR), which measures the electrical conductance of the skin, can be used as a measurable parameter reflecting stress and other emotional states [5], [6]. Automatic detection of user's emotional state can be useful for applications in which humans and machines interact, particularly in human-machine collaborative systems, where systems can adapt to human's emotional state. GSR signal has two components, the tonic level of skin conductance referred to as skin conductance level (SCL), and rapid phasic responses referred to as skin conductance responses (SCRs) [4]. An example of a typical GSR signal is presented in Fig. 1. SCL varies slowly and it is continuously changing. SCRs appear as accentuated peaks and may or may not be related to stimulus events. They are characterized by a minimum amplitude of $0.01 \ \mu S$ (micro Siemens) and a latency value between 1-3 $s$, a rise time value between 1-3 $s$ and half recovery time value between 2-10 $s$ with an exponential decay [4], [7]. The skin conductance response can be elicited by a specific stimulus (S-SCR) or elicited spontaneously, that is, without any identifiable stimulus, referred to as non-specific SCR (NS-SCRs). The number of NS-SCRs peaks elicited in a given time period (frequency) is typically 1-3 per/min in rest periods and over 20 per/min in high arousal situations [7]. GSR and other physiological signals such as body temperature and heart rate, also controlled by the ANS, have been used in real world applications to detect emotional arousal. Healey and Picard [8] explored different biosignals (e.g. electrocardiogram, electromyogram, GSR) during real world driving tasks in order to detect driver's stress levels (low, medium, high). They recorded data during rest periods and while driving in the highway and in the busy main street. These data were divided into 5-minute segments and then classified in the 3 stress levels. They showed that the most relevant information to distinguish these stress levels

is obtained through skin conductivity and heart rate metrics. GSR was also used in computer-based arithmetic and reading tasks [9], [10] to measure users performance and cognitive load. Most of the works analyze the GSR signal in laboratory conditions, pointing out possible applications, but without actually using GSR to influence or change the behaviour of the system.

This paper analyzes whether GSR activity, recorded in participants steering a robotic wheelchair with a BCI, is elicited in particular contexts susceptible of triggering emotional arousals such as stress. Additionally, it is researched whether GSR can be automatically detected to adapt a human-machine collaborative controller. Healthy and motor impaired participants were asked to steer the RobChair ISR-UC prototype [3] in indoor office environments (which include narrow doors, circumventing obstacles). Emotional state recognition can be applied in several contexts. For example, if a high level of stress is detected, the BCI can be automatically adjusted, by increasing the time for command detection; or RobChair's navigation system can take full control, disregarding user's input commands. Thus, the system could be able to adapt according to both navigation context and user's state, increasing the overall system reliability.

The main contributions of this paper are: 1) A novel method FBPD to detect SCRs, based on peak detection and exponential fitting; 2) Analysis of GSR recorded while a robotic wheelchair is steered in real-time with a BCI; and 3) Validation with motor impaired participants.

## II. EXPERIMENTAL DESIGN

### A. Navigation Experiments

Participants underwent two experiments where they were asked to steer RobChair in indoor office environment using a self-paced P300-based BCI (Fig. 2). P300 is an event related potential that appears in response of a relevant and rare stimuli (target event) in an oddball paradigm. In a self-paced operation, the BCI detects automatically when the user is willing or not to send a command, i.e., it identifies a control state or a non-control state. RobChair is a differential robotic wheelchair, eqquiped with optical encoders and an hokuyo UTM-30LX laser scan. Its navigation architecture is implemented in ROS, being composed of: a SLAM module; an hybrid motion planner [3], and a collaborative controller that receives commands from the P300-based BCI.

The experiments consisted of two navigation tasks with travelled distances around 59 m and 48 m respectively. In the first task (Fig. 3 a)) users had to go from START to END, passing three narrow doorways (B, I and K), avoiding two small (D and F) and two big obstacles (E and G). The second task consisted in steering RobChair from START to the elevator (Fig. 3 b)). This route included two narrow doorways (B and D), one obstacle (G) and an unexpected trajectory (remote take over) of RobChair near the elevator. When users were approaching the elevator, they were asked to provide a FORWARD command, but a remote operator took control of RobChair, without users' knowledge, changing the command to BACK causing RobChair to move backwards.
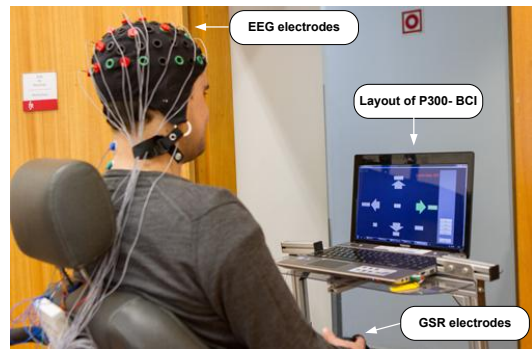


Fig. 2.   A snapshot taken during an online experiment when RobChair is passing through a narrow door.

### B. Participants and Biosignals Acquisition

The experiments were performed by seven able-bodied participants, two participants with cerebral palsy (CP), one participant with agenesis of the four members, one participants with spinal cord injuries (SCI), one participant with limb-girdle muscular dystrophy and one participant with Duchenne muscular dystrophy (DMD). Each participant or parent responsible gave informed consent to participate in the study. The consent form contains the description and purpose of the research, the experimental procedure, the potential risks and the permission to publish the results. The group of able-bodied participants with ages from 21 to 32 years old, averaging 23.7 years old are referred to as group I (GI). The motor disabled participants referred to as group II (GII) are aged between 21 and 50 years old, with a mean age of 37.5 years old.

The electroencephalographic (EEG) and GSR signals were recorded with a 16-channel g.USBamp bioamplifier. The EEG signals were recorded with active Ag/AgCl electrodes at positions Fz, Cz, C3, C4, CPz, Pz, P3, P4, PO7, PO8, POz and Oz according to the international extended 10-20 standard system. The electrodes were referenced to the right or left earlobe and the ground was the AFz electrode. The GSR signals were captured from the index and middle fingers of non-dominant hand using the g.GSRsensor2. All signals were sampled at 256 Hz and filtered using a 50 Hz notch filter. EEG signals were filtered by a 0.1-30 Hz band-pass filter and GSR signals were filtered by a low-pass filter with 1Hz cutoff frequency.

## III. METHODOLOGY

### A. Self-paced P300-BCI Paradigm

The BCI comprises a set of seven possible commands: FORWARD, BACK, LEFT90, RIGHT90, STOP, WC, and EXIT (see Fig. 2). The words associated with these commands flash randomly, with the same probability. The desired command is called the target event (oddball stimulus) and the remaining options are the standard events. The symbols flash with a duration of 100 $ms$ and an inter-stimulus interval of 75 $ms$. The number of rounds ($N_{rep}$) was settled considering a P300 offline accuracy around 90% (obtained
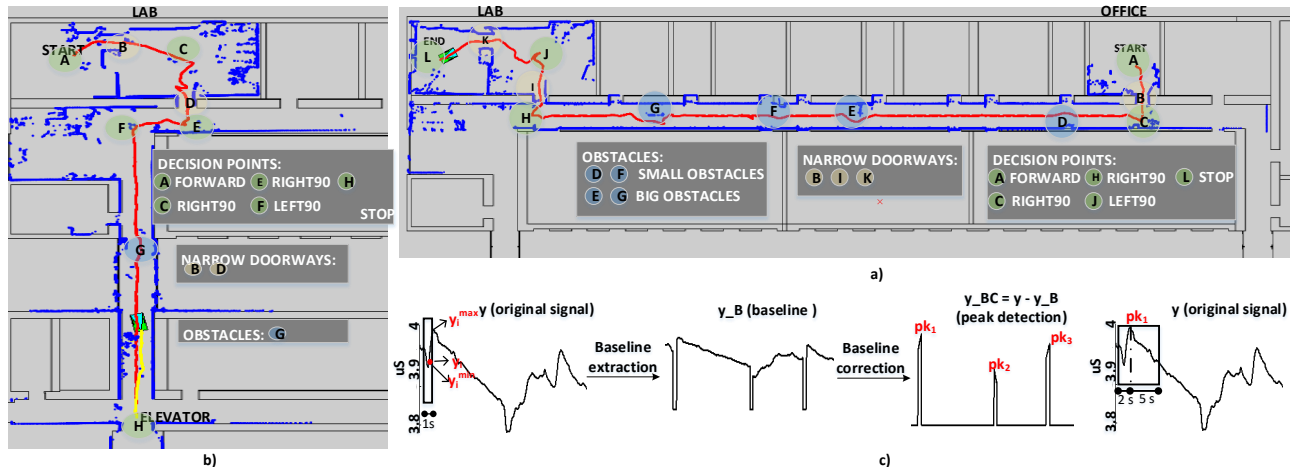
Fig. 3. a) First navigation task with 4 obstacles, 3 narrow passages and 5 decision points (where users have to provide a command). The red line corresponds to the path performed by RobChair, and blue line represents the laser scan data. b) Second navigation task with one obstacle, 2 narrow passages, 5 decision points and remote control to create an unexpected trajectory of the RobChair (yellow line). c) SCRs peaks detection. First, a sliding window of 1-second is used to detect baseline points on signal $y$, then peaks are detected from baseline corrected signal ($y\_BC$). A sliding window of 7-seconds is used to verify if peak $pk$ in signal $y$ has an amplitude higher than 0.01 $\mu S$ and if it has an exponential decay.

from a calibration session). The time of one trial (set of rounds) is calculated as:

$$TT = N_{rep} \times N_s \times SOA + CT \qquad (1)$$

where $N_s = 7$ is the number of symbols, $SOA = 175ms$ is the stimuli onset asynchrony and $CT = 1s$ is the time associated with the last flash of the trial. Participants were instructed to focus on the desired command and ignore the remaining standard symbols. Before the online session, the calibration phase was performed in order to collect data to train the classifier (using the same framework of [11]). The calibration session took about 3 minutes gathering 72 target epochs and 432 non-target epochs. During the online session, participants controlled RobChair in real-time, providing commands in decision points (see Fig. 3 a) and Fig. 3 b)) and whenever necessary to deal with specific situations (e.g. when RobChair stopped because someone was walking in the corridors).

### B. SCR Detection

Several approaches have been used to extract SCRs from GSR. Greco et al. [12] consider the GSR signal as the sum of three components: phasic, tonic, and noise and use a convex optimization approach (cvxEDA) to split these 3 components. Then, the area of the phasic component is computed and a signal with area exceeding a 0.5 threshold is considered a SCR. In [13] a median filter is applied and subtracted from the signal to remove the SCL component (baseline). In the phasic data, the SCRs are detected based on a threshold for the peak onset and a threshold for the peak offset ($< 0\mu S$). Given that SCL is continuously moving, methods based on baseline correction are the most effective for SCR detection.

We propose a baseline correction inspired in [14] (usually used for correction of baseline distortion in spectra), and then we fit specific characteristics of typical SCRs signals

(amplitude and exponential decay) to each possible SCR peak. We call the proposed method feature-based peak detection (FBPD). Let us consider the GSR signal represented by $y$ (see Fig. 3 c)). To decide if a point $y(i)$ belongs to the baseline, a sliding window of 1-second-width is centred at each time sample $i$. Then, the minimum and maximum values ($y_i^{min}$ and $y_i^{max}$) are computed for each window. If their difference is less than a threshold value ($TH$), the point $y(i)$ is considered part of the baseline. The baseline signal ($y_B$) is constructed from

$$y_B = \begin{cases} y(i), & \text{if } y_i^{max} - y_i^{min} < TH \\ c, & \text{otherwise} \end{cases} \qquad (2)$$

The threshold is $TH = n \times \sigma_{noise}$, where $\sigma_{noise}$ is the noise standard deviation and $n$ is usually set between 2 and 4. In our experiments it was empirically adjusted to 4. To compute the $\sigma_{noise}$, the signal $y$ is divided into 32 equal regions. Then, the standard deviation $\sigma$ of each region is calculated and $\sigma_{noise}$ is the one with minimum value. The constant $c$ is the minimum value of GSR signal for each participant obtained during the rest period (before the onset of the experiment).

Then, the baseline curve is subtracted from the GSR signal resulting in the baseline corrected signal $y_{BC} = y - y_B$, clearly revealing the peaks ($pk$) associated with SCRs. Matching the instants of the detected peaks on signal $y$ and using a rise time value of 2 $s$ and a half recovery time of 5 $s$ we compute the amplitude of each peak as the difference between maximum and minimum of the window. We fit the data window with an exponential $a \times e^{-bx}$. If $a > 0$, $0 < b < 1$ and the amplitude is greater than 0.01 $\mu S$, the peak is considered a SCR, otherwise it is discarded. The algorithm is flexible, since it uses two characteristics of the SCR (amplitude and exponential decay), which can be adjusted.
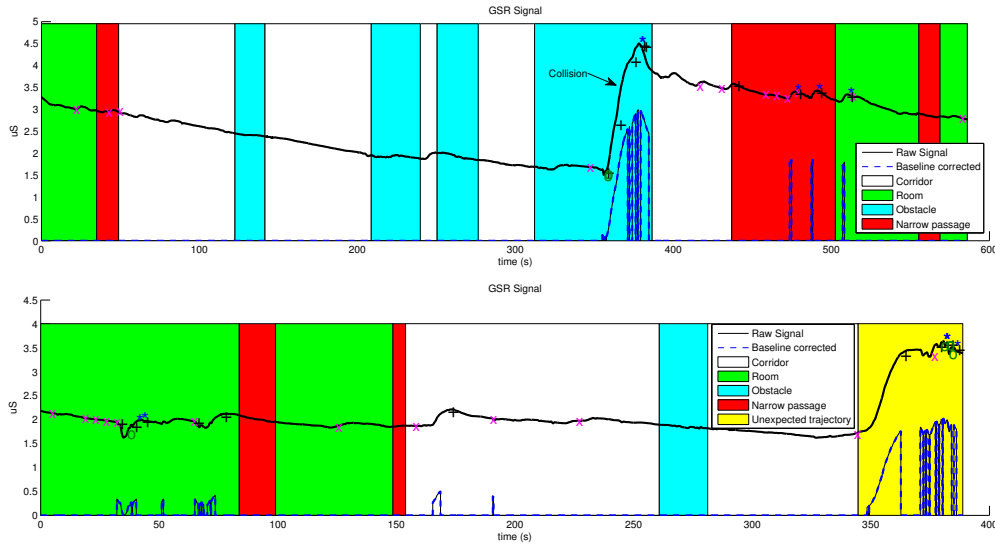
Fig. 4. GSR signal during first (top) and second (bottom) navigation task. Plots contain low-pass-filtered GSR signal (solid line), GSR signal after baseline correction (dashed line), peaks detected by our algorithm (marked with ∗), peaks detected by the median filter (marked with +), peaks detected by cvxEDA methods (marked with o) and BCI commands (marked with ×).

TABLE I

NUMBER OF SCRs ELICITED DURING THE EXPERIMENTS

| | Narrow passages | | Obstacles | | Unexpected trajectories | | Rooms and corridors | | Automatic detection accuracy (%) | | Collisions[a] |
|---|---|---|---|---|---|---|---|---|---|---|---|
| | GI (35) | GII (20) | GI (35) | GII (20) | GI (7) | GII (4) | GI | GII | GI | GII | GI (3) |
| SCRs detected manually | 33 | 18 | 43 | 27 | 22 | 17 | 143 | 112 | | | 3 |
| SCRs detected using proposed FBPD | 28 | 19 | 34 | 22 | 25 | 16 | 172 | 128 | 82.4 | 87.6 | 3 |
| SCRs detected using median filter | 38 | 11 | 52 | 19 | 33 | 14 | 226 | 60 | 69.3 | 32.7 | 3 |
| SCRs detected using cvxEDA | 15 | 16 | 34 | 11 | 30 | 27 | 76 | 121 | 33.3 | 78.9 | 1 |
| Amplitude ($\mu S$) | 0.3 | 0.3 | 0.2 | 0.3 | 1.0 | 0.9 | 0.7 | 0.5 | | | 1.7 |
| Frequency (per/min) | 2.1 | 2.4 | 1.9 | 2.0 | 4.2 | 4.9 | 1.6 | 2.0 | | | |

[a]During the navigation tasks performed by GI, 3 collisions (slight lateral scraping) occurred and all of them elicited one SCR. For GII there were no collisions.

TABLE II

NUMBER OF EVENTS THAT ELICITED AT LEAST ONE SCR

| | Narrow passages | | Obstacles | | Unexpected trajectories | | Collisions | |
|---|---|---|---|---|---|---|---|---|
| | GI (35) | GII (20) | GI (35) | GII (20) | GI (7) | GII (4) | GI (3) | GII (0) |
| SCRs detected manually | 17 | 9 | 19 | 12 | 6 | 4 | 3 | - |
| SCRs detected using proposed FBPD | 14 | 11 | 16 | 9 | 7 | 4 | 3 | - |
| SCRs detected using median filter | 20 | 7 | 19 | 6 | 7 | 3 | 3 | - |
| SCRs detected using cvxEDA | 4 | 5 | 7 | 4 | 4 | 3 | 3 | - |
| SCRs elicited (%) | 48.6 | 45.0 | 54.3 | 60.0 | 85.7 | 100.0 | 100.0 | - |

## IV. EXPERIMENTAL RESULTS AND DISCUSSION

### A. Analysis of GSR Signal in Stressful Situations

The experiments were carried out by seven healthy participants (Group I - GI) and six motor disabled participants (Group II - GII), however the results of two motor disabled participants were discarded, one because there was no electrodermal response, and the other because of strong artifact contamination. Participants steered RobChair with the self-paced P300-based BCI on two distinct routes. The BCI accuracy was 97.1% and 96.4% in group GI, respectively for the first and the second route, with an average time per command $TT = 6.7s$. Group GII achieved a BCI accuracy of 95.6% and 94.9% for the first and second routes with a $TT = 6.2s$.

Examples of RobChair routes and relevant points are marked in maps of Fig. 3 a) and Fig. 3 b). Routes, decision points and events were recorded synchronously with GSR and EEG. In Fig. 4, we show the complete GSR recording

for a representative able-bodied participant during the first and the second navigation tasks, as well as the navigation events labelled as follows: corridors (white), rooms (green), obstacles (blue), narrow passages (red), and the unexpected RobChair trajectory (yellow). There were also some slight lateral scrapings on obstacles, which are marked in Fig. 4 as collisions. Black solid line represents the preprocessed lowpass-filtered GSR signal and the blue dashed line represents the GSR signal after baseline correction. Baseline correction makes significant peaks evident, enabling the detection of S-SCRs and NS-SCRs. Fig. 4 shows that a strong SCR was elicited when a lateral collision with an obstacle G occurred, while no SCRs were elicited when RobChair passed previous obstacles without collisions. The first and third narrow passages did not elicit any SCRs and the second narrow passage elicited some SCRs. In the second navigation task (bottom of Fig. 4) there is a well-defined SCR with high amplitude originated by an unexpected trajectory, resulting from the remote operation of RobChair without participant knowledge.

The automatic detection of GSR was evaluated through the proposed FBPD method, the median filter approach [13], and the convex optimization approach [12], considering the visual detection of a human expert as ground truth. The human detection, although susceptible of misclassification, provides the most reliable reference for the validation of the automatic methods. Fig. 4 shows the SCRs detected by the 3 automatic detectors. We assumed as S-SCRs all peaks that occurred in narrow passages, obstacles, collisions and unexpected RobChair trajectories, and as NS-SCRs all peaks that occurred in rooms and corridors. The 3 algorithms are user-independent, that is, the model parameters are the same for all participants. The median filter has only one adjustable parameter, the width of the window, which was set to 4 $s$ centered on the current sample. We evaluated the cvxEDA method with the same parameters defined in [12]. Table I shows the number of S-SCRs and NS-SCRs detected manually and by the automatic algorithms. The classification accuracy was respectively 82.4%, 69.3% and 33.3% for GI and 87.6%, 32.7% and 78.9% for GII. The FBPD method performed better than the other two with a classification accuracy above 82% for both groups. These results show that detecting SCRs based on exponential fitting as proposed in FBPD is more effective than the approaches based on peak and area thresholds. The median filter and cvxEDA methods [12], [13] had irregular performance, with a tendency to overestimate the number of detected peaks in one group and underestimate in the other group. The amplitude and frequency of S-SCRs and NS-SCRs are known to be related to stress level. Table I shows these two parameters, taking the SCRs detected with FBPD. The frequency of S-SCRs elicited in collisions was not calculated since collisions occurred during very brief periods of time. The SCRs elicited in narrow passages and obstacle contour had lower amplitudes than the SCRs that occurred in rooms and corridors, and their frequencies were typical of NS-SCRs (1-3 per/min) [7]. Therefore, we can conclude that
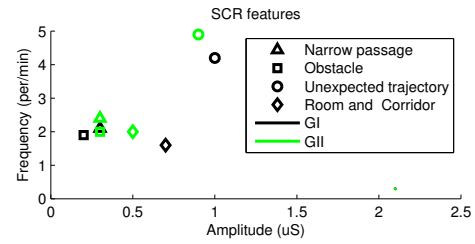


Fig. 5. Scatter plot of average frequency vs average amplitude of SCRs in different events.

narrow passages and obstacles did not affect participants. Collision and unexpected trajectory were the events eliciting the SCRs with the highest amplitude and frequency. These two situations show clear evidence of users' arousal, i.e., the participants were very sensitive to sudden events. Figure 5 illustrates well these conclusions. The unexpected trajectories event is discriminated at the top right corner. Collision events are not represented, because they are very brief and therefore impossible to measure the SCR frequency.

Table II shows the percentage of events that elicited at least one SCR. For GI, we found that 17 narrow passages, 19 obstacles, 3 collision and 6 unexpected trajectory elicited at least one SCR. Collisions elicited SCRs in 100% of the times, and the unexpected trajectories of RobChair resulted in SCRs in 87.5% of the times. However, SCRs were elicited in only 48.6% of narrow passages and 54.3% of obstacles. For GII we verified similar results, SCRs were elicited in 100.0% of unexpected trajectories and in only 45.0% of narrow passages and 60.0% of obstacles. For GI, 76.5% of SCRs elicited in narrow passages and 100.0% of SCRs elicited in obstacles occurred on the first task. For GII 78.8% and 75.0% of SCRs elicited in narrow passages and bypassing obstacles occurred on the first task. These results could mean that the participants gained confidence in RobChair in the first task, reducing their emotional arousal in the second task.

The presence of NS-SCRs increase the difficulty in associating SCRs to stressful events. Most of state-of-the-art applications use SCRs features (e.g., peak rate, peak height, response durations) disregarding the discrimination between SCRs and NS-SCRs. For a system that aims to self-adjust to user's emotional arousals the non-discrimination between S-SCRs and NS-SCRs may be critical. As shown in Fig. 5, amplitude and frequency of peaks can be used to adjust a threshold for distinguishing both. In the future, other SCR features such as rise time and area under the responses could be explored in order to increase the discrimination between S-SCR and NS-SCR.

### B. Relationship Between SCRs and BCI Performance

An analysis was carried out to investigate whether information of SCRs can be used to anticipate wrong BCI commands and if wrong commands led to an increase of SCRs. We analyzed the last 4 $s$ and 60 $s$ before each BCI command and the 60 $s$ after the commands. The participants of GI and GII performed the two navigation tasks with 143 and 91 correct BCI commands and 13 and 10 wrong

TABLE III

NUMBER OF CORRECT BCI COMMANDS THAT ELICITED AT LEAST ONE SCR

| | Correct BCI commands - GI: 143 and GII: 91 | | | | | |
| | Period of 4 $s$ before a BCI command | | Period of 60 $s$ before a BCI command | | Period of 60 $s$ after a BCI command | |
| | GI | GII | GI | GII | GI | GII |
| SCRs detected using proposed FBPD | 26 | 11 | 91 | 75 | 88 | 77 |
| Percentage of commands that elicited SCRs | 18.2 | 12.1 | 63.6 | 82.4 | 61.5 | 84.6 |

TABLE IV

NUMBER OF WRONG BCI COMMANDS THAT ELICITED AT LEAST ONE SCR

| | Wrong BCI commands - GI: 13 and GII: 10 | | | | | |
| | Period of 4 $s$ before a BCI command | | Period of 60 $s$ before a BCI command | | Period of 60 $s$ after a BCI command | |
| | GI | GII | GI | GII | GI | GII |
| SCRs detected using proposed FBPD | 5 | 0 | 11 | 8 | 11 | 9 |
| Percentage of commands that elicited SCRs | 38.5 | 0.0 | 84.6 | 80.0 | 84.6 | 90.0 |

BCI commands, respectively (Table III and Table IV). The wrong commands were preceded by a percentage of SCRs higher than the correct commands for group GI. However, for group GII the percentage of SCRs for correct and wrong commands was similar. Therefore, we could not establish a clear relationship between SCRs and BCI performance that could be used to anticipate a BCI error. Comparing the percentage of commands that elicited SCRs before and after correct and wrong commands, we verify that the percentage is similar for correct commands and that it is higher after wrong commands in group GII. The results suggest that BCI errors could have caused emotional arousal in group GII.

## V. CONCLUSIONS

In this paper, the GSR was analyzed to infer whether it could be reliably correlated to stressful situations, and automatically detected while users were driving a brain-actuated RobChair. SCRs were elicited in 87.5% and 100% of times in unexpected RobChair trajectories respectively for GI and GII groups, and in 100% of lateral collisions for both groups. These results demonstrated that information of SCR may be used to detect stressful situations. The method FBPD proposed for automatic detection of SCRs proved to be very effective comparing to state of the art methods. Despite the encouraging results, the lack of clear discrimination between S-SCR and NS-SCR hampers the identification of stressful situations. The correlation between SCRs and BCI performance was inconclusive and a set of experiments is being prepared to further research this correlation.

## ACKNOWLEDGMENT

## REFERENCES

[1] A. C. Lopes, G. Pires, and U. Nunes, "Assisted navigation for a brain-actuated intelligent wheelchair," *Rob Auton Syst*, vol. 61, no. 3, pp. 245–258, 2013.

[2] T. Carlson and J. d. R. Millan, "Brain-controlled wheelchairs: a robotic architecture," *IEEE Robot Autom Mag*, vol. 20, no. 1, pp. 65–73, 2013.

[3] A. Lopes, J. Rodrigues, J. Perdigao, G. Pires, and U. Nunes, "A new hybrid motion planner: Applied in a brain-actuated robotic wheelchair," *IEEE Robot Autom Mag*, vol. 23, no. 4, pp. 82–93, 2016.

[4] M. E. Dawson, A. M. Schell, and D. L. Filion, "The electrodermal system," *Handbook of psychophysiology*, vol. 2, pp. 200–223, 2007.

[5] S. Cornelia, F. Gravenhorst, J. Schumm, B. Arnrich, and G. Tröster, "Towards long term monitoring of electrodermal activity in daily life," *Personal and Ubiq Comp Journ*, 2013.

[6] C. Setz, B. Arnrich, J. Schumm, R. La Marca, G. Tröster, and U. Ehlert, "Discriminating stress from cognitive load using a wearable eda device," *IEEE Trans Inf Technol Biomed*, vol. 14, no. 2, pp. 410–417, 2010.

[7] W. Boucsein, *Electrodermal activity*. Springer Science & Business Media, 2012.

[8] J. A. Healey and R. W. Picard, "Detecting stress during real-world driving tasks using physiological sensors," *IEEE trans Intell Transp Syst*, vol. 6, no. 2, pp. 156–166, 2005.

[9] C. Mundell, J. P. Vielma, and T. Zaman, "Predicting performance under stressful conditions using galvanic skin response," *arXiv preprint arXiv:1606.01836*, 2016.

[10] N. Nourbakhsh, Y. Wang, F. Chen, and R. A. Calvo, "Using galvanic skin response for cognitive load measurement in arithmetic and reading tasks," in *Proc of the 24th Australian Computer-Human Interaction Conf.* ACM, 2012, pp. 420–423.

[11] G. Pires, U. Nunes, and M. Castelo-Branco, "Statistical spatial filtering for a p300-based bci: tests in able-bodied, and patients with cerebral palsy and amyotrophic lateral sclerosis," *J Neurosci Methods*, vol. 195, no. 2, pp. 270–281, 2011.

[12] A. Greco, G. Valenza, A. Lanata, E. P. Scilingo, and L. Citi, "cvxeda: A convex optimization approach to electrodermal activity processing," *IEEE Trans Biomed Eng*, vol. 63, no. 4, pp. 797–804, 2016.

[13] iMotions, "Galvanic skin response the complete pocket guide," *iMotions Biometric Research*, 2017.

[14] S. Golotvin and A. Williams, "Improved baseline recognition and modeling of ft nmr spectra," *J of Magn Reson*, vol. 146, no. 1, pp. 122–125, 2000.